Hindawi Publishing Corporation
EURASIP Journal on Wireless Communications and Networking
Volume 2007, Article ID 68563, 10 pages
doi:10.1155/2007/68563

Research Article

Joint Compensation of OFDM Frequency-Selective Transmitter and Receiver IQ Imbalance

Deepaknath Tandur and Marc Moonen

ESAT-SCD (SISTA), Departement Elektrotechniek, Katholieke Universiteit Leuven, Kasteelpark Arenberg 10, 3001 Leuven-Heverlee, Belgium

Received 21 November 2006; Revised 14 March 2007; Accepted 24 May 2007

Recommended by Richard Kozick

Direct-conversion architectures are recently receiving a lot of interest in OFDM-based wireless transmission systems. However, due to component imperfections in the front-end analog processing, such systems are very sensitive to in-phase/quadrature-phase (IQ) imbalances. The IQ imbalance results in intercarrier interference (ICI) from the mirror carrier of the OFDM symbol. The resulting distortion can limit the achievable data rate and hence the performance of the system. In this paper, the joint effect of frequency-selective IQ imbalance at both the transmitter and receiver ends is studied. We consider OFDM transmission over a time-invariant frequency-selective channel. When the cyclic prefix is long enough to accommodate the channel impulse response combined with the transmitter and receiver filters, we propose a low-complexity two-tap equalizer with LMS-based adaptation to compensate for IQ imbalances along with channel distortions. When the cyclic prefix is not sufficiently long, then in addition to ICI there also exists interblock interference (IBI) between the adjacent OFDM symbols. In this case, we propose a frequency domain per-tone equalizer (PTEQ) obtained by transferring a time-domain equalizer (TEQ) to the frequency domain. The PTEQ is initialized by a training-based RLS scheme. Both algorithms provide a very efficient post-FFT adaptive equalization and their performance is shown to be close to the ideal case.

1. INTRODUCTION

Orthogonal frequency division multiplexing (OFDM) is a popular, standardized modulation technique for broadband wireless systems: it is used for wireless LAN [1], fixed broadband wireless access [2], digital video & audio broadcasting [3], and so forth.

Hence, a lot of effort is spent in developing integrated, cost-and power-efficient OFDM transmission and reception systems. The zero-IF architecture (or direct-conversion architecture) is an attractive candidate as it can convert the RF signal directly to baseband or vice versa without any intermediate frequencies (IF). This results in an overall smaller size with lower component cost as compared to a traditional superheterodyne architecture. However, the zero-IF architecture performs the in-phase/quadrature-phase (IQ) modulation and demodulation in the analog domain. This inherent two-path analog processing results in the system being extremely sensitive to mismatches between the I and Q branch, especially so when high-order modulations schemes (e.g., 64 QAM, etc.) are used. Due to component imperfections in practical analog electronics, such imbalances are unavoidable, resulting in an overall performance degradation of the system.

Generally, the IQ imbalance introduced by the local oscillator (LO) of the front end can be considered constant over the signal bandwidth. Such IQ imbalances are considered frequency independent. However, the mismatch introduced by the preceding or subsequent IQ branch amplifiers and filters tends to vary with frequency. Such frequency-dependent or frequency-selective IQ imbalance is particularly severe in wide-band direct-conversion transmitters and receivers. Rather than decreasing the IQ imbalance by increasing the design time and the component cost of the analog processing, IQ imbalance can also be tolerated and then compensated digitally.

The performance degradation due to receiver IQ imbalance in OFDM systems has been investigated in [4, 5]. Several compensation algorithms considering either only receiver IQ imbalance or transmitter IQ imbalance have been developed in [6–9], and so forth. Recently, joint compensation algorithms for frequency independent (constant over frequency)

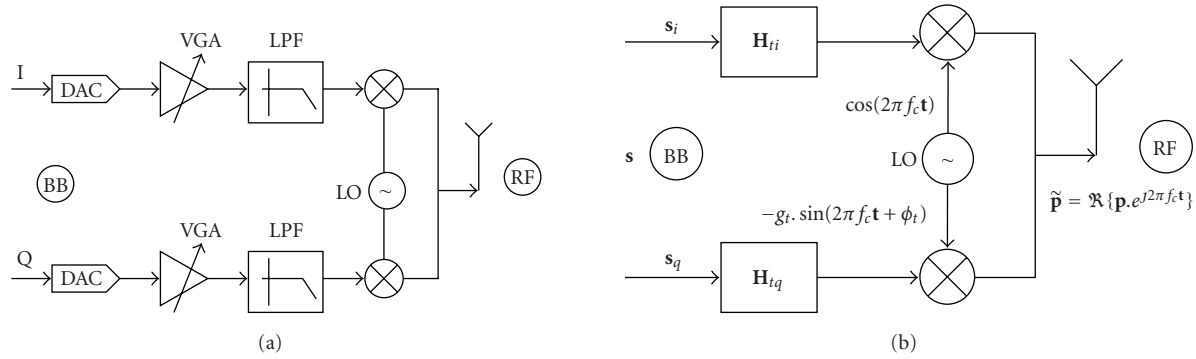

Figure 1: (a) Direct-conversion transmitter. (b) Mathematical model of a direct-conversion transmitter.

transmitter and receiver IQ imbalance have been proposed in [10]. In [11], a compensation scheme for frequency-selective transmitter and receiver IQ imbalance is developed but the scheme is very complex due to the large number of equalizers and taps per equalizer needed, which also results in a slow convergence.

In this paper, the joint effect of frequency-selective IQ imbalance at both the transmitter and receiver ends is studied. When the cyclic prefix is long enough to accommodate the combined channel, transmitter and receiver filter impulse response, we propose a low-complexity two-tap equalizer with LMS-based adaptation. Due to the small number of taps needed, the algorithm converges faster and provides a better performance as will be demonstrated. When the cyclic prefix is not sufficiently long, there will be inter-block Interference (IBI) between adjacent OFDM symbols. In this case a simple two-tap adaptive equalizer is not sufficient to preserve the carrier orthogonality. We propose a frequency domain per-tone equalizer (PTEQ) [12] which shortens the combined impulse response to fit within the cyclic prefix and at the same time compensates for the imperfection of the analog front end. The PTEQ can be trained by an RLS adaptive scheme. The present research is an extension of our previous work [13, 14] where various compensation techniques for joint transmitter and receiver frequency-independent IQ imbalance under carrier frequency offset (CFO) have been developed.

This paper is organized as follows. In Section 2, we develop a model for joint transmitter and receiver frequency-selective IQ imbalance in an OFDM transmission system. In Section 3, the basics of a suitable compensation scheme are explained. Section 4 presents the adaptive compensation algorithms used. Simulation results are shown in Section 5 and finally conclusions are given in Section 6.

2. IQ IMBALANCE MODEL

The following notation is adopted in the description of the system. Vectors are indicated in bold and scalar parameters in normal font. Superscripts $*$, T, H represent conjugate, transpose, and hermitian, respectively. $\mathbf{F}$ and $\mathbf{F}^{-1}$ represent the $N \times N$ discrete Fourier transform and its inverse. $\mathbf{I}_N$ is the $N \times N$ identity matrix and $0_{M\times N}$ is the $M \times N$ all zero matrix. Operators $\otimes$, $\star$, and $\cdot$ denote Kronecker product, convolution and component-wise vector multiplication, respectively.

Let $\mathbf{S}^{(i)}$ be a frequency domain complex OFDM symbol of size $(N \times 1)$ where i is the time index of the symbol. For our data model we consider two successive OFDM symbols transmitted at time $i-1$ and i, respectively. The ith symbol is the symbol of interest, the previous symbol is used to model the IBI. These symbols are transformed to the time domain by the inverse discrete Fourier transform (IDFT). A cyclic prefix (CP) of length ν is then added to the head of each symbol. In the case of no IQ imbalance in the front end of the transmitter, the resulting time domain baseband signal is given as follows:

$$\mathbf{s} = (\mathbf{I}_2 \otimes \mathbf{P})(\mathbf{I}_2 \otimes \mathbf{F}^{-1}) \begin{bmatrix} \mathbf{S}^{(i-1)} \\ \mathbf{S}^{(i)} \end{bmatrix}, \tag{1}$$

where $\mathbf{P}$ is the cyclic prefix insertion matrix given by

$$\mathbf{P} = \left[\begin{array}{c|c} 0_{(\nu\times N-\nu)} & \mathbf{I}_\nu \\ \hline & \mathbf{I}_N \end{array}\right]. \tag{2}$$

The direct conversion transmitter is shown in Figure 1(a) and its mathematical model is represented in Figure 1(b). We categorize the IQ imbalance resulting from the front-end as frequency dependent and frequency independent. The imbalances caused by digital-to-analog converters (DAC), amplifiers, low pass filters (LPFs), and mixers generally result in an overall frequency-dependent IQ imbalance. We represent this imbalance at the transmitter by two mismatched filters with frequency responses given as $\mathbf{H}_{ti}$ and $\mathbf{H}_{tq}$. As the LO produces only a single tone, the IQ imbalance caused by the LO can be generally categorized as frequency independent over the signal bandwidth with a transmitter amplitude and phase mismatch g_t and ϕ_t between the two branches.

Let $\tilde{\mathbf{p}}$ be the transmitted signal given as

$$\tilde{\mathbf{p}} = \Re\{\mathbf{p} \cdot e^{j2\pi f_c \mathbf{t}}\}, \tag{3}$$

where $\mathbf{p} = \mathbf{p}_i + J\mathbf{p}_q$ is the baseband equivalent signal of $\tilde{\mathbf{p}}$. Note that we apply a vector function notation, where the (exponential) function is applied to each component of the vector $\mathbf{t}$.

Following the derivation in [8], the baseband signal $\mathbf{p}$ can be given as

$$\mathbf{p} = \mathbf{g}_{t1} \star \mathbf{s} + \mathbf{g}_{t2} \star \mathbf{s}^*, \tag{4}$$

where

$$\begin{aligned} \mathbf{g}_{t1} &= \mathbf{F}^{-1}\{\mathbf{G}_{t1}\} = \mathbf{F}^{-1}\left\{\frac{[\mathbf{H}_{ti} + g_t e^{-j\phi_t}\mathbf{H}_{tq}]}{2}\right\}, \\ \mathbf{g}_{t2} &= \mathbf{F}^{-1}\{\mathbf{G}_{t2}\} = \mathbf{F}^{-1}\left\{\frac{[\mathbf{H}_{ti} - g_t e^{j\phi_t}\mathbf{H}_{tq}]}{2}\right\}. \end{aligned} \tag{5}$$

Here $\mathbf{g}_{t1}$ and $\mathbf{g}_{t2}$ are mostly truncated to length L_t and then padded with $N - L_t$ zero elements. They represent the combined frequency-independent and dependent transmitter IQ imbalance. The convolution operations will be specified as matrix-vector products further up. Note also that $\mathbf{g}_{t2}$ vanishes if $g_t = 1$, $\phi_t = 0$, and $\mathbf{H}_{ti} = \mathbf{H}_{tq}$.

We now consider OFDM transmission over a time-invariant frequency-selective channel. Let $\mathbf{c}$ be the impulse response of the multipath channel of length L. The channel adds a filtering in formula (4), so that the received baseband signal $\mathbf{r}$ can be given as

$$\begin{aligned} \mathbf{r} &= \mathbf{c} \star \mathbf{p} + \mathbf{v} = \mathbf{c} \star \mathbf{g}_{t1} \star \mathbf{s} + \mathbf{c} \star \mathbf{g}_{t2} \star \mathbf{s}^* + \mathbf{v} \\ &= \mathbf{c}_1 \star \mathbf{s} + \mathbf{c}_2 \star \mathbf{s}^* + \mathbf{v}, \end{aligned} \tag{6}$$

where $\mathbf{c}_1$ and $\mathbf{c}_2$ are the combined transmitter IQ and channel impulse responses of length $L + L_t - 1$ and $\mathbf{v}$ is the additive white Gaussian noise (AWGN).

Finally, an expression similar to (4) can be used to model IQ imbalance at the receiver. Let $\mathbf{z}$ represent the down-converted baseband complex signal after being distorted by combined frequency dependent and independent receiver IQ imbalance $\mathbf{g}_{r1}$ and $\mathbf{g}_{r2}$ of length L_r. Then $\mathbf{z}$ will be given as

$$\mathbf{z} = \mathbf{g}_{r1} \star \mathbf{r} + \mathbf{g}_{r2} \star \mathbf{r}^*. \tag{7}$$

Equation (6) can be substituted in (7) leading to

$$\begin{aligned} \mathbf{z} &= \left(\mathbf{g}_{r1} \star \mathbf{c}_1 + \mathbf{g}_{r2} \star \mathbf{c}_2^*\right) \star \mathbf{s} \\ &\quad + \left(\mathbf{g}_{r1} \star \mathbf{c}_2 + \mathbf{g}_{r2} \star \mathbf{c}_1^*\right) \star \mathbf{s}^* + \tilde{\mathbf{v}} \\ &= \mathbf{d}_1 \star \mathbf{s} + \mathbf{d}_2 \star \mathbf{s}^* + \tilde{\mathbf{v}}, \end{aligned} \tag{8}$$

where $\mathbf{d}_1$ and $\mathbf{d}_2$ are the combined transmitter IQ, channel and receiver IQ impulse responses of length $L_t + L + L_r - 2$ and $\tilde{\mathbf{v}}$ is the additive noise which is also modified by the receiver imbalances.

Substituting (1) in (8), we obtain

$$\begin{aligned} \mathbf{z} &= \left[\mathbf{O}_1 \mid \mathbf{T}_{d1}\right](\mathbf{I}_2 \otimes \mathbf{P})(\mathbf{I}_2 \otimes \mathbf{F}^{-1}) \begin{bmatrix} \mathbf{S}^{(i-1)} \\ \mathbf{S}^{(i)} \end{bmatrix} \\ &\quad + \left[\mathbf{O}_1 \mid \mathbf{T}_{d2}\right](\mathbf{I}_2 \otimes \mathbf{P})(\mathbf{I}_2 \otimes \mathbf{F}^{-1}) \begin{bmatrix} \mathbf{S}_m^{*(i-1)} \\ \mathbf{S}_m^{*(i)} \end{bmatrix} + \tilde{\mathbf{v}}, \end{aligned} \tag{9}$$

where $\mathbf{z}$ is of dimension $(N \times 1)$, $\mathbf{O}_1 = 0_{(N\times N+2\nu-L_T-L-L_r+3)}$. $\mathbf{T}_{dk}$ (for $k = 1, 2$) is an $(N \times N + L_t + L + L_r - 3)$ Toeplitz matrix with first column $[\mathbf{d}_{k(L_t+L+L_r-3)}, 0_{(1\times N-1)}]^T$ and first row $[\mathbf{d}_{k(L_t+L+L_r-3)}, \ldots, \mathbf{d}_{k(0)}, 0_{(1\times N-1)}]$. Here $()_m$ denotes the mirroring operation in which the vector indices are reversed such that $\mathbf{S}_m[l] = \mathbf{S}[l_m]$

$$\text{where } \begin{cases} l_m = 2 + N - l & \text{for } l = 2 \cdots N, \\ l_m = l & \text{for } l = 1. \end{cases} \tag{10}$$

If the impulse responses $\mathbf{d}_1$ and $\mathbf{d}_2$ are shorter than the OFDM cyclic prefix ($\nu \geq L_t + L + L_r - 2$), then (8) can be given in the frequency domain as

$$\begin{aligned} \mathbf{Z} &= \mathbf{D}_1 \cdot \mathbf{S}^{(i)} + \mathbf{D}_2 \cdot \mathbf{S}_m^{*(i)} + \tilde{\mathbf{V}} \\ &= \left(\mathbf{G}_{r1} \cdot \mathbf{G}_{t1} \cdot \mathbf{C} + \mathbf{G}_{r2} \cdot \mathbf{G}_{t2m}^* \cdot \mathbf{C}_m^*\right) \cdot \mathbf{S}^{(i)} \\ &\quad + \left(\mathbf{G}_{r1} \cdot \mathbf{G}_{t2} \cdot \mathbf{C} + \mathbf{G}_{r2} \cdot \mathbf{G}_{t1m}^* \cdot \mathbf{C}_m^*\right) \cdot \mathbf{S}_m^{*(i)} + \tilde{\mathbf{V}}, \end{aligned} \tag{11}$$

where $\mathbf{Z}$, $\mathbf{D}_1$, $\mathbf{D}_2$, $\mathbf{G}_{r1}$, $\mathbf{G}_{r2}$, $\mathbf{C}$, and $\tilde{\mathbf{V}}$ are frequency domain representations of $\mathbf{z}$, $\mathbf{d}_1$, $\mathbf{d}_2$, $\mathbf{g}_{r1}$, $\mathbf{g}_{r2}$, $\mathbf{c}$, and $\tilde{\mathbf{v}}$.

Equation (11) shows that due to the transmitter and receiver IQ imbalance, power leaks from the signal on the mirror carrier ($\mathbf{S}_m^*$) to the carrier under consideration ($\mathbf{S}$) and thus causes inter-carrier interference (ICI). Note that if no IQ imbalance is present, then $g_t = g_r = 1$, $\phi_t = \phi_r = 0$, $\mathbf{H}_{ti} = \mathbf{H}_{tq} = \mathbf{H}_t$, $\mathbf{H}_{ri} = \mathbf{H}_{rq} = \mathbf{H}_r$. Thus $\mathbf{G}_{t1} = \mathbf{H}_t$, $\mathbf{G}_{r1} = \mathbf{H}_r$, and $\mathbf{G}_{t2} = 0$, $\mathbf{G}_{r2} = 0$ leading to the baseband signal $\mathbf{Z} = \mathbf{H}_t \cdot \mathbf{H}_r \cdot \mathbf{C} \cdot \mathbf{S}^{(i)}$, that is, a scaled version of $\mathbf{S}^{(i)}$ with no ICI. As OFDM is very sensitive to ICI, IQ imbalance may result in a severe performance degradation. This is illustrated in Section 5.

If the OFDM cyclic prefix is not sufficiently long ($\nu < L_t + L + L_r - 2$), then (11) will no longer hold true. In addition to ICI from the mirror carrier $\mathbf{S}_m^{(i)}$, there will be interferences from the adjacent OFDM symbol $\mathbf{S}^{(i-1)}$ leading to IBI. This IBI can be compensated by a per-tone equalizer (PTEQ), which can be obtained by transferring two time-domain equalizers (TEQs) to the frequency domain. In the next section, a PTEQ-based IQ compensation technique is derived first, and then the compensation scheme for the sufficiently long cyclic prefix case is derived merely by simplifying the equations.

3. IQ IMBALANCE COMPENSATION

To shorten the combined channel, transmitter and receiver filter impulse responses $\mathbf{d}_1$ and $\mathbf{d}_2$ such that they fit within the cyclic prefix, a traditional (single) time-domain equalizer (TEQ) is not sufficient. We propose to use two TEQs $\mathbf{w}_1$ and $\mathbf{w}_2$ where one is applied to the received signal ($\mathbf{z}_1 = \mathbf{z}$) and the other to the conjugated version of the received signal ($\mathbf{z}_2 = \mathbf{z}^*$). Adding the second TEQ generally leads to a better combined shortening of $\mathbf{d}_1$ and $\mathbf{d}_2$.

Let L' be the number of taps used in each TEQ $\mathbf{w}_1$ and $\mathbf{w}_2$, then the size of the distorted received symbol $\mathbf{z}$ in (9) has to be adjusted to $(N + L' - 1 \times 1)$. Hence, $\mathbf{O}_1 = 0_{(N+L'-1\times N+2\nu-L-L_T-L_r-L'+4)}$, $\mathbf{T}_{dk}$ (for $k = 1, 2$) is of size $(N + L' - 1 \times N + L_t + L + L_r + L' - 4)$ with first column $[\mathbf{d}_{k(L_t+L+L_r-3)}, 0_{(1\times N+L'-1)}]^T$ and first row $[\mathbf{d}_{k(L_t+L+L_r-3)}, \ldots, \mathbf{d}_{k(0)}, 0_{(1\times N+L'-2)}]$. In conjunction with the

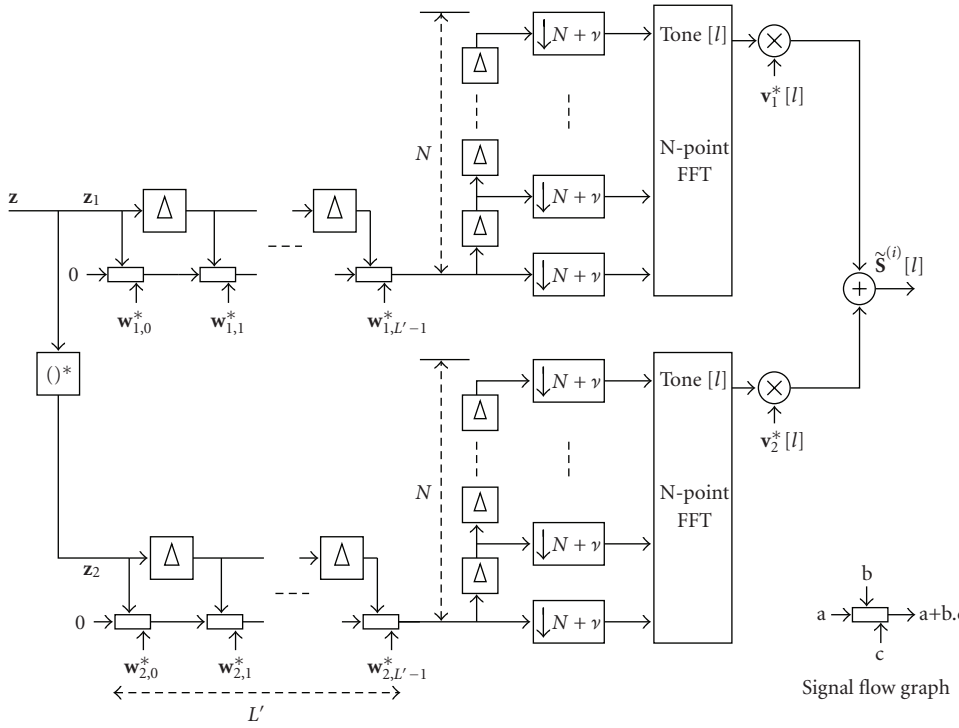

Figure 2: L' tap TEQs with 2-tap FEQ per tone.

TEQ-based channel shortening, a DFT is applied to the filtered sequences $\mathbf{z}_1$ and $\mathbf{z}_2$. Finally, a two-tap frequency-domain equalizer (FEQ) is applied to recover the transmitted OFDM symbol. This scheme is shown in Figure 2.

We define $\widetilde{\mathbf{S}}^{(i)}[l]$ as the estimate for lth subcarrier of the ith OFDM symbol. This estimate is then obtained as

$$\widetilde{\mathbf{S}}^{(i)}[l] = \mathbf{v}_1^*[l] \cdot (\mathbf{F}[l]\mathbf{W}_1^H\mathbf{z}_1) + \mathbf{v}_2^*[l] \cdot (\mathbf{F}[l]\mathbf{W}_2^H\mathbf{z}_2), \quad (12)$$

where $\mathbf{v}_1[l]$ and $\mathbf{v}_2[l]$ are the taps of FEQ operating on the lth subcarrier, and $\mathbf{F}[l]$ is the lth row of the DFT matrix $\mathbf{F}$. $\mathbf{W}_k$ (for $k = 1, 2$) is an $(N + L' - 1 \times N)$ Toeplitz matrix with first column $[\mathbf{w}_{k,L'-1}, \ldots, \mathbf{w}_{k,0}, 0_{(1\times N-1)}]$ and first row $[\mathbf{w}_{k,L'-1}, 0_{(1\times N-1)}]$.

Following the derivation in [12], the two TEQs thus obtained can be transformed to the frequency domain resulting in two per-tone equalizers (PTEQs) each employing one DFT and $L' - 1$ difference terms. With this transformation the difficult channel shortening problem is avoided and replaced by simple per-tone optimization problem. Equation (12) is then modified as follows:

$$\widetilde{\mathbf{S}}^{(i)}[l] = \mathbf{v}_1^H[l]\mathbf{F}_i[l]\mathbf{z}_1 + \mathbf{v}_2^H[l]\mathbf{F}_i[l]\mathbf{z}_2, \quad (13)$$

where $\mathbf{v}_k[l]$ for $k = 1, 2$ are PTEQs of size $(L' \times 1)$. $\mathbf{F}_i[l]$ is defined as

$$\mathbf{F}_i[l] = \left[\begin{array}{c|c|c} \mathbf{I}_{L'-1} & 0_{L'-1\times N-L'+1} & -\mathbf{I}_{L'-1} \\ \hline 0_{1\times L'-1} & \mathbf{F}[l] & \end{array}\right], \quad (14)$$

where the first block row in $\mathbf{F}_i[l]$ is seen to extract the difference terms, while the last row corresponds to the single DFT.

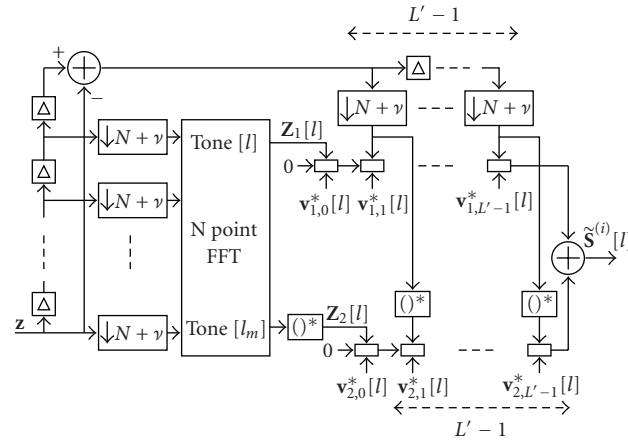

Figure 3: PTEQ for OFDM with IQ imbalance.

As $\mathbf{z}_2 = \mathbf{z}_1^* = \mathbf{z}^*$, the PTEQ structure is further simplified by taking only one DFT whose conjugated output in reverse order corresponds to $\mathbf{Z}_2 = \mathbf{F}\{\mathbf{z}_2\} = \mathbf{F}\{\mathbf{z}_1^*\} = \mathbf{Z}_{1m}^*$. The resulting PTEQ block scheme is shown in Figure 3.

The PTEQ coefficients for the lth subcarrier can be obtained based on the following MSE minimization:

$$\min_{(\mathbf{v}_1[l],\mathbf{v}_2[l])} \mathbb{E}\left\{ \left| \mathbf{S}^{(i)}[l] - \left[\mathbf{v}_1^H[l] \;\; \mathbf{v}_2^H[l]\right] \left[\begin{array}{c} \mathbf{F}_i[l]\mathbf{z}_1 \\ \mathbf{F}_i[l]\mathbf{z}_2 \end{array}\right] \right|^2 \right\}, \quad (15)$$

where $\mathbb{E}\{\cdot\}$ is the expectation operator.

For the case of a sufficiently long cyclic prefix ($\nu \geq L_t + L + L_r - 2$), we may consider a PTEQ of order $L' = 1$. In this case, (11) for $\mathbf{Z}_2 = \mathbf{Z}_m^*$ and $\mathbf{Z}_1 = \mathbf{Z}$ can be written in matrix form for each carrier as follows:

$$\begin{bmatrix} \mathbf{Z}_1[l] \\ \mathbf{Z}_2[l] \end{bmatrix} = \begin{bmatrix} \mathbf{D}_1[l] & \mathbf{D}_2[l] \\ \mathbf{D}_{2m}^*[l] & \mathbf{D}_{1m}^*[l] \end{bmatrix} \begin{bmatrix} \mathbf{S}^{(i)}[l] \\ \mathbf{S}_m^{*(i)}[l] \end{bmatrix} + \begin{bmatrix} \widetilde{\mathbf{V}}[l] \\ \widetilde{\mathbf{V}}_m^*[l] \end{bmatrix}. \tag{16}$$

From this it follows that for the noiseless case, the desired signal $\mathbf{S}^{(i)}[l]$ can be obtained by taking an appropriate linear combination of $\mathbf{Z}_1[l]$ and $\mathbf{Z}_2[l]$, that is,

$$\begin{aligned} &\begin{bmatrix} \mathbf{v}_1^*[l] & \mathbf{v}_2^*[l] \end{bmatrix} \begin{bmatrix} \mathbf{Z}_1[l] \\ \mathbf{Z}_2[l] \end{bmatrix} \\ &\quad = \underbrace{\begin{bmatrix} \mathbf{v}_1^*[l] & \mathbf{v}_2^*[l] \end{bmatrix} \begin{bmatrix} \mathbf{D}_1[l] & \mathbf{D}_2[l] \\ \mathbf{D}_{2m}^*[l] & \mathbf{D}_{1m}^*[l] \end{bmatrix}}_{\begin{bmatrix} 1 & 0 \end{bmatrix}} \begin{bmatrix} \mathbf{S}^{(i)}[l] \\ \mathbf{S}_m^{*(i)}[l] \end{bmatrix} \\ &\quad \Longrightarrow \mathbf{S}^{(i)}[l] = \begin{bmatrix} \mathbf{v}_1^*[l] & \mathbf{v}_2^*[l] \end{bmatrix} \begin{bmatrix} \mathbf{Z}_1[l] \\ \mathbf{Z}_2[l] \end{bmatrix}. \end{aligned} \tag{17}$$

This formula demonstrates that a receiver structure can be designed that exactly compensates for the transmitter and receiver IQ imbalance and the channel effect (i.e., zero-forcing (ZF) equalization). The coefficients $\mathbf{v}_1$ and $\mathbf{v}_2$ can be computed from $\mathbf{G}_{t1}$, $\mathbf{G}_{t2}$, $\mathbf{G}_{r1}$, $\mathbf{G}_{r2}$, and $\mathbf{C}$, if these are available. In the noisy case a suitable set of coefficients can be estimated based on an MSE minimization:

$$\min_{(\mathbf{v}_1[l], \mathbf{v}_2[l])} \mathbb{E}\left\{ \left| \mathbf{S}^{(i)}[l] - \begin{bmatrix} \mathbf{v}_1^*[l] & \mathbf{v}_2^*[l] \end{bmatrix} \begin{bmatrix} \mathbf{Z}_1[l] \\ \mathbf{Z}_2[l] \end{bmatrix} \right|^2 \right\} \tag{18}$$

which is a special case ($L' = 1$) of the more general formula (15).

In the next section a training-based initialization of $\mathbf{v}_1$ and $\mathbf{v}_2$ is described, based on such an MMSE criterion.

4. ADAPTIVE COMPENSATION

For the case ($\nu < L_t + L + L_r - 2$), we consider RLS-based initialization of the PTEQ coefficients based on (15). The RLS algorithm provides optimal convergence and achieves initialization with an acceptably small number of training symbols. Let d be the number of OFDM symbols dedicated for training. The RLS algorithm to compute the coefficient vector for subcarrier l is shown in Algorithm 1. Let $\mathbf{v}_1^{(i)}[l]$ and $\mathbf{v}_2^{(i)}[l]$ represent the equalization vectors at time instant i. The regularization factor δ is a small positive constant and $\mathbf{D}^{(i)}$ is the training symbol transmitted at time instant i.

Algorithm 1 (RLS direct equalization). Initialize the algorithm by setting

$$\begin{aligned} \mathbf{v}_1^{(i=0)} &= 0_{L' \times N}, \\ \mathbf{v}_2^{(i=0)} &= 0_{L' \times N}. \end{aligned} \tag{19}$$

For all the carriers in OFDM symbol $l = 1 \cdots N$, compute

$$\mathbf{B}^{(i=0)} = \delta^{-1} \mathbf{I}_{2L' \times 2L'}. \tag{20}$$

For each iteration $i = 1 \cdots d$, compute

$$\begin{aligned} \mathbf{u}^{(i)}[l] &= \begin{bmatrix} \mathbf{F}_i[l]\mathbf{z}_1^{(i)} & \mathbf{F}_i[l]\mathbf{z}_2^{(i)} \end{bmatrix}^T, \\ \xi^{(i)} &= \mathbf{D}^{(i)}[l] - \begin{bmatrix} \mathbf{v}_1^{H(i-1)}[l] & \mathbf{v}_2^{H(i-1)}[l] \end{bmatrix} \mathbf{u}^{(i)}[l] \\ \mathbf{B}_1^{(i)} &= \frac{\mathbf{B}^{(i)}\mathbf{u}^{(i)}[l]}{1 + \mathbf{u}^{H(i)}[l]\mathbf{B}^{(i)}\mathbf{u}^{(i)}[l]} \\ \mathbf{v}_1^{(i)}[l] &= \mathbf{v}_1^{(i-1)}[l] + \left(\mathbf{B}_{1,(1\cdots L')}^{(i)} \xi^{*(i)}\right)^T, \\ \mathbf{v}_2^{(i)}[l] &= \mathbf{v}_2^{(i-1)}[l] + \left(\mathbf{B}_{1,(L'+1\cdots 2L')}^{(i)} \xi^{*(i)}\right)^T, \\ \mathbf{B}^{(i)} &= \mathbf{B}^{(i-1)} - \mathbf{B}_1^{(i-1)} \mathbf{u}^{H(i)}[l] \mathbf{B}^{(i-1)}. \end{aligned} \tag{21}$$

At the end of the training the weights $\mathbf{v}_1[l]$ and $\mathbf{v}_2[l]$ are substituted in formula (13) to obtain the transmitted symbol estimates $\widetilde{\mathbf{S}}^{(i)}[l]$.

In the case ($\nu \geq L_t + L + L_r - 2$), a single LMS equalizer with two taps per OFDM carrier is sufficient for compensation with close to optimal performance. The solution proposed reduces to the same solution as in [9] where only frequency-selective receiver IQ imbalance is considered. But due to the presence of joint frequency-selective transmitter and receiver IQ imbalance, the distortion is more severe and hence larger number of training symbols is needed for adequate compensation. This is also illustrated in Figure 4.

The two inputs of the equalizer are $\mathbf{Z}_1[l]$ and $\mathbf{Z}_2[l]$. The taps $\mathbf{v}_1[l], \mathbf{v}_2[l]$ are trained using k training symbols based on (18). The symbol estimate $\widetilde{\mathbf{S}}^{(i)}$ at the output of the equalizer can be written as

$$\widetilde{\mathbf{S}}^{(i)}[l] = \mathbf{v}_1^{*(i)}[l] \cdot \mathbf{Z}_1^{(i)}[l] + \mathbf{v}_2^{*(i)}[l] \cdot \mathbf{Z}_2^{(i)}[l], \quad i = 1 \cdots k. \tag{22}$$

The equalization coefficients are updated according to the LMS rule:

$$\begin{aligned} \mathbf{v}_1^{(i+1)}[l] &= \mathbf{v}_1^{(i)}[l] + \mu \mathbf{e}^{*(i)}[l] \cdot \mathbf{Z}_1^{(i)}[l], \\ \mathbf{v}_2^{(i+1)}[l] &= \mathbf{v}_2^{(i)}[l] + \mu \mathbf{e}^{*(i)}[l] \cdot \mathbf{Z}_2^{(i)}[l], \end{aligned} \tag{23}$$

where $\mathbf{e}^{(i)}[l] = \mathbf{D}^{(i)}[l] - \widetilde{\mathbf{S}}^{(i)}[l]$ is the error signal generated at iteration i for the tone index l using a training symbol $\mathbf{D}^{(i)}[l]$ and μ is the LMS step-size parameter. In a decision-directed adaptation, $\mathbf{D}^{(i)}[l]$ is a decision based on $\widetilde{\mathbf{S}}^{(i)}[l]$, in which case the convergence may be slower. Once the equalizer coefficients are trained with a suitable number of training symbols, the obtained coefficients are used to equalize the received signal according to (22).

Equations (22) and (23) show that to update the equalizer weights, 3 multiplications and 3 additions are needed, whereas to equalize a single carrier 2 multiplications and 1 addition is needed. The equalizer coefficients can be updated once every OFDM symbol. In the case of IEEE 802.11a where data is transmitted on 48 out of 64 tones, 48 equalizers will

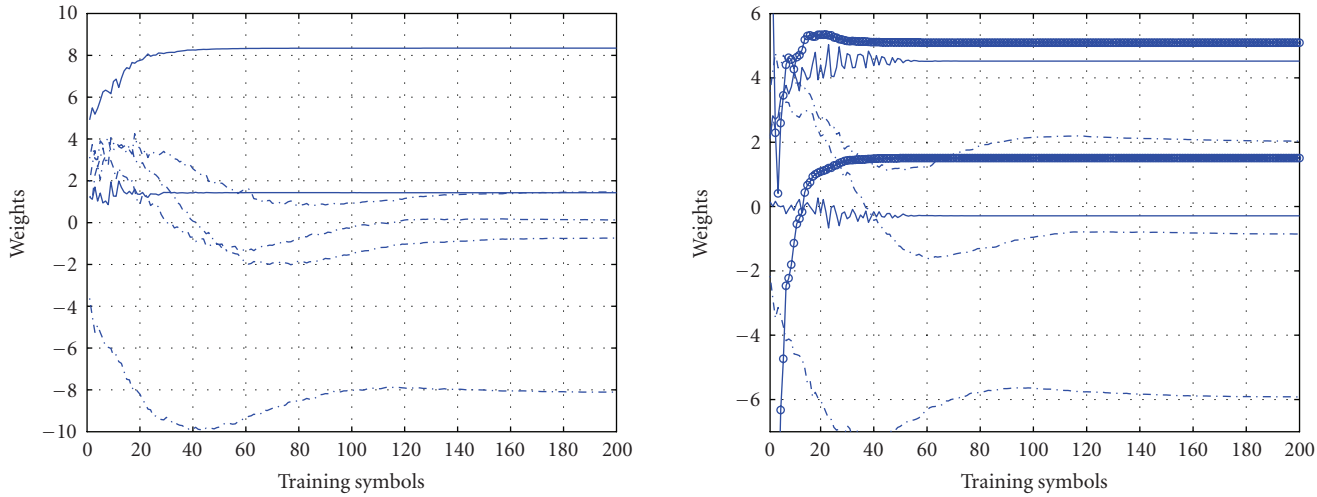

(a) Frequency-dependent IQ imbalance

(b) Frequency-dependent and independent IQ imbalance

Figure 4: Equalizer convergence speed for 64 QAM constellation in noiseless scenario. The dark curves represent equalizer weights of the proposed 2-tap adaptive scheme in the case of IQ imbalance at both the transmitter and receiver ends. Dark curves with circles represent equalizer weights of the proposed 2-tap adaptive scheme in the case of IQ imbalance only at the receiver end. Dotted curves represent equalizer weights in the scheme of [11] in the case of IQ imbalance at both the transmitter and receiver ends. Frequency-independent amplitude imbalance of $g_t, g_r = 3\%$ and phase imbalance of $\phi_t, \phi_r = 3^\circ$. The front-end filter impulse responses are $\mathbf{h}_{ti} = [1, 0.5]$, $\mathbf{h}_{tq} = [0.9, 0.2]$, and $\mathbf{h}_{ri} = [1, 0.5]$, $\mathbf{h}_{rq} = [0.9, 0.2]$

be needed. Table 1 compares the computational load of our algorithm and the one mentioned in [11] for such systems.

From the table we observe that the proposed algorithm has a significantly reduced complexity. This is mainly because fewer taps are needed per equalizer. Having fewer taps also allows for faster convergence and hence the overall performance can be improved. Figure 4 illustrates the equalizer convergence in the noiseless multipath channel scenario when both frequency-dependent and independent IQ imbalance exist in the system. We consider a 64 QAM constellation system, a frequency-independent amplitude imbalance of $g_t, g_r = 3\%$, and phase imbalance of $\phi_t, \phi_r = 3^\circ$ at both transmitter and receiver. In the frequency-dependent case, the filter impulse responses are $\mathbf{h}_{ti} = [1, 0.5]$, $\mathbf{h}_{tq} = [0.9, 0.2]$, and $\mathbf{h}_{ri} = [1, 0.5]$, $\mathbf{h}_{rq} = [0.9, 0.2]$. The multipath channel is of length $L = 4$ taps chosen independently from a complex Gaussian distribution and the cyclic prefix length $\nu = 8$ is sufficiently long here. The dotted curves correspond to the four equalizer weights in the scheme of [11] and the dark curves correspond to two equalizer weights of our method. In Figure 4(b), the dark curves with circles also correspond to two equalizer weights of our method when there is frequency-dependent and independent IQ imbalance only at the receiver end. As can be observed from the figure, due to the smaller number of taps needed in our scheme, the convergence is significantly faster. For the case of only frequency-dependent transmitter and receiver IQ imbalance, the weights converge after 30 symbols, while it takes around 50 symbols to achieve good convergence in the case of combined frequency-dependent and independent transmitter and receiver IQ imbalance. For the case of only receiver IQ imbalance, it takes around 30 symbols for convergence. Thus a good compensation can be achieved with fewer training symbols when IQ imbalance exists only at the receiver end. In the scheme of [11], the four weights converge after 125 symbols for frequency-dependent transmitter and receiver IQ imbalance and after 140 symbols for the combined frequency-dependent and independent transmitter and receiver IQ imbalance.

Table 1: Comparison of computation load.

Algorithm in [11]		Proposed algorithm	
Equalizer update	Equalization	Equalizer update	Equalization
288 mul	384 mul	144 mul	96 mul
288 add	288 mul	144 add	48 mul

5. SIMULATION RESULTS

A typical OFDM system (similar to IEEE 802.11a) is simulated to evaluate the performance of the compensation scheme for transmitter and receiver IQ imbalance. The end-to-end OFDM system model with an LMS equalizer for the case when the cyclic prefix is sufficiently long, that is, $(\nu \geq L_t + L + L_r - 2)$ is shown in Figure 5. The colored boxes are the front ends of the communication system where IQ imbalances are introduced. For the case of insufficient cyclic prefix length $(\nu < L_t + L + L_r - 2)$, the compensation block shown in the figure is replaced by the PTEQ block of Figure 3.

The parameters used in the simulation are as follows: the OFDM symbol length is $N = 64$, cyclic prefix length is $\nu = 8$. Similar results can be obtained for $\nu = 16$ when the combined channel and front-end filter impulses are longer. We

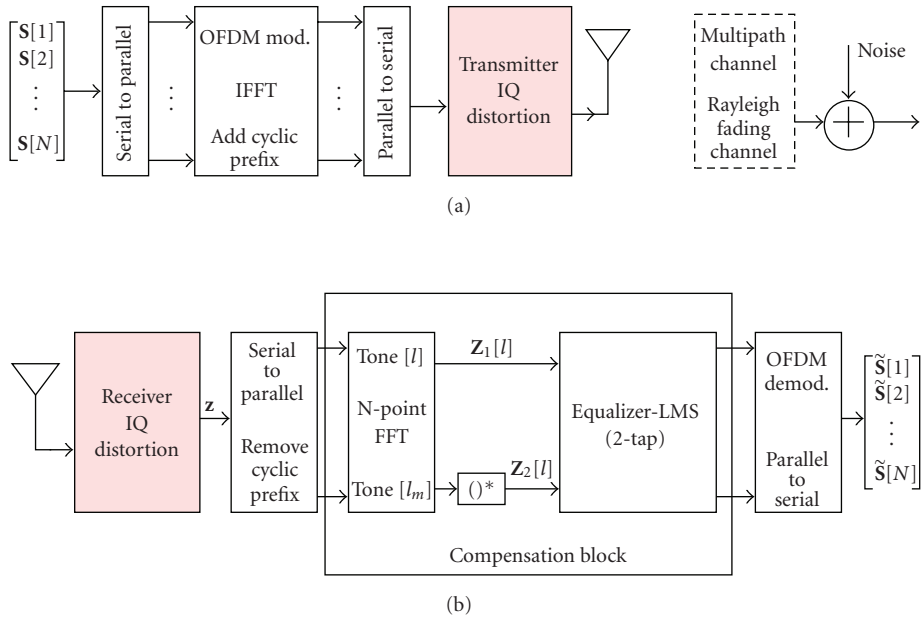

Figure 5: Imbalance model for the analog front-end including frequency dependent and independent IQ imbalance.

consider a frequency-independent amplitude imbalance of $g_t, g_r = 5\%$ and phase imbalance of ϕ_t, $\phi_r = 5^\circ$ at both the transmitter and receiver. In the frequency-dependent imbalance case the front-end filter impulse response are $\mathbf{h}_{ti} = [0.9, 0.1]$, $\mathbf{h}_{tq} = [0.1, 0.9]$, and $\mathbf{h}_{ri} = [0.9, 0.1]$, $\mathbf{h}_{rq} = [0.1, 0.9]$. Thus the front-end filter impulse length is $L_t = L_r = 2$. It should be noted that the imbalance level in this case may be higher than the level observed in a practical receiver. However, we consider such an extreme case to evaluate the robustness/effectiveness of the proposed compensation scheme.

There are three different channel profiles: (1) an additive white Gaussian noise (AWGN) channel with a single-tap unity gain. (2) A multipath channel with $L = 4$ taps. In both the cases 1 and 2, $(L_t + L + L_r - 2 < \nu)$ and a simple 2-tap LMS equalizer can be used for compensation. The step size μ of the LMS equalizer is initially set to 0.35 and is dynamically reduced as the simulation progresses. (3) A multipath channel with $L = 10$ taps. In this case $(L_t + L + L_r - 2 > \nu)$, and an RLS-based adaptive PTEQ with $L' = 10$ and $L' = 15$ taps is used for compensation. The taps of multipath channel are chosen independently with complex Gaussian distribution. The convergence can be improved further by estimating the channel separately on initial training symbols as is done normally in 802.11a. This shortens the convergence period but an adaptive equalizer is still needed to equalize the channel and the IQ imbalance.

Figure 6 shows the performance curves, that is, (BER versus SNR) obtained for an uncoded 64 QAM OFDM system in the presence of frequency-dependent and independent IQ imbalance. Every channel realization is independent of the previous one and the BER results depicted are obtained by averaging the BER curves over 10^4 independent channels. Figures 6(a), 6(b), and 6(d) consider the presence of IQ imbalance at both transmitter and receiver ends while Figure 6(c) considers IQ imbalance only at receiver end. The performance comparison is made with an ideal system with no front-end distortion and with a system with no IQ compensation algorithm included. In addition Figures 6(c) and 6(d) also compare the PTEQ equalizer of length $L' = 10$ and $L' = 15$ with a PTEQ equalizer of length $L' = 1$ which is equivalent to the simple LMS compensation scheme. With no compensation scheme in place, the OFDM system is completely unusable. Even for the case when there is only frequency-independent IQ imbalance, the BER is very high. For the case $(L_t + L + L_r - 2 < \nu)$, close to ideal performance is obtained with the simple LMS compensation scheme in place. For the case $(L_t + L + L_r - 2 > \nu)$, good performance is obtained when PTEQ length $L' = 15$. This is also shown in Table 2 where the performance (BER loss in dB) of PTEQ equalizer with different tap lengths L' is compared with the ideal case at SNR $= 42$ dB. When $L' = 1$, that is, LMS equalization case, even with no IQ imbalance at both transmitter and receiver ends, the BER loss is very high and is approximately 2.77 dB higher than the ideal case. When IQ imbalance is present only at receiver end the loss is about 7.6 dB and when the IQ imbalance is present at both transmitter and receiver ends the BER loss increases to 9.26 dB. The PTEQ performance improves when the number of taps is increased but this is at the expense of higher complexity. For a PTEQ of tap-length $L' = 15$, in the case of no IQ imbalance at both transmitter and receiver ends, the BER loss is 0.25 dB. When IQ imbalance is present only at receiver end, the BER loss is 0.83 dB and with IQ imbalance at both transmitter and receiver ends the BER loss increases only marginally to 1.09 dB. This can also be observed from Figures 6(c) and 6(d), where the BER performance curve for $L' = 15$ is very close to the ideal case. Thus a PTEQ with a sufficient number of taps is essential to shorten the combined channel, transmitter and

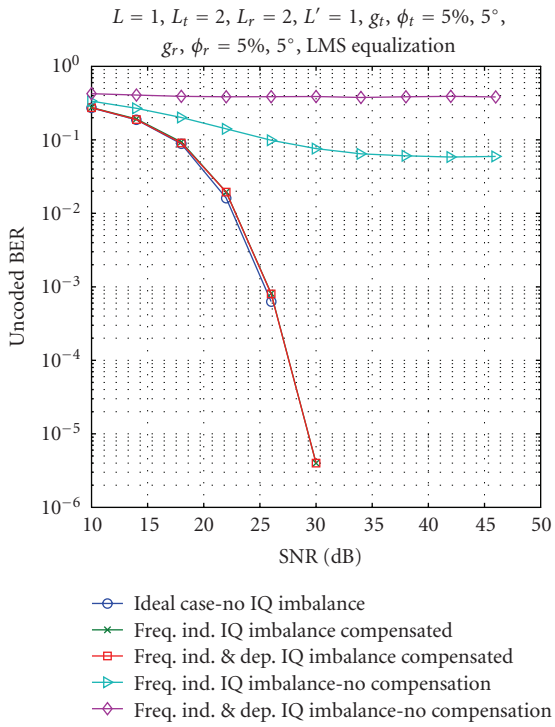

(a) AWGN flat channel (nonfading) with IQ imbalance at both transmitter and receiver ends

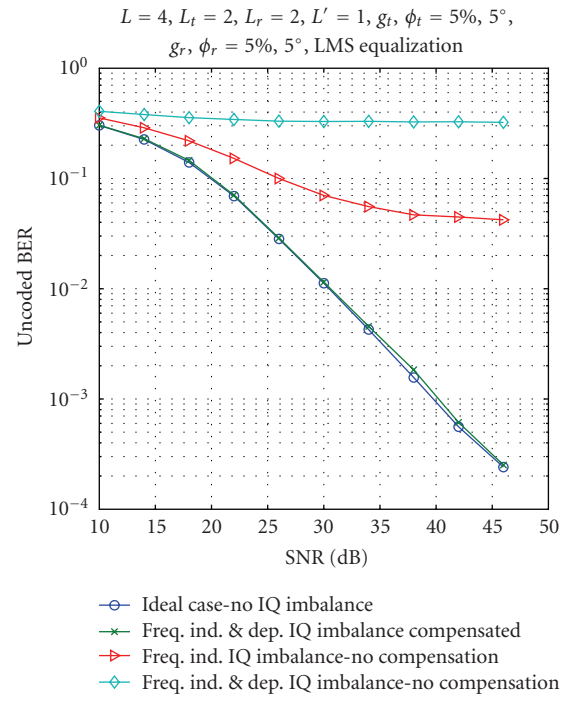

(b) 4-tap Rayleigh fading channel (fading) with IQ imbalance at both transmitter and receiver ends

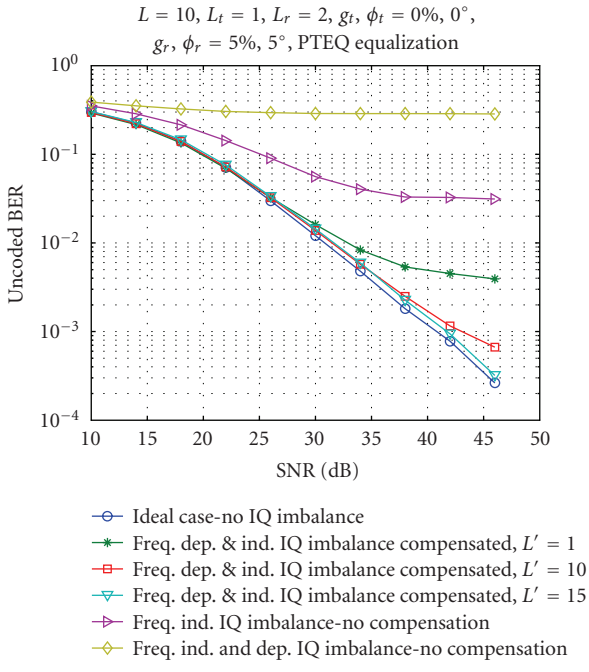

(c) 10-tap Rayleigh fading channel (fading) with IQ imbalance only at receiver end

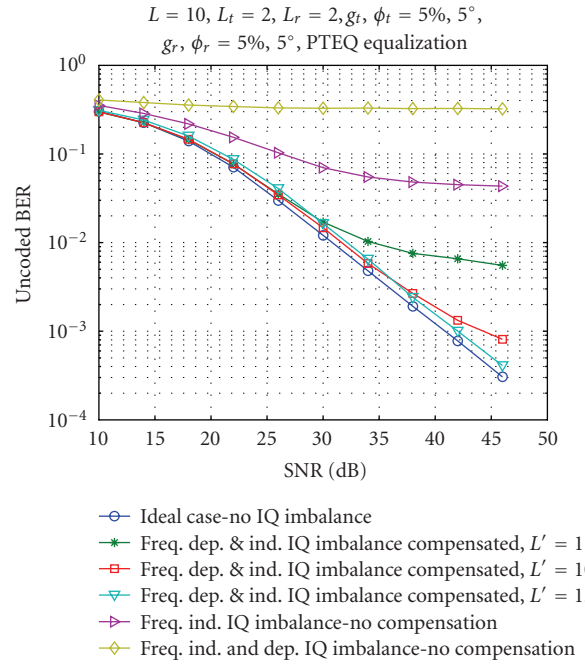

(d) 10-tap Rayleigh fading channel (fading) with IQ imbalance at both transmitter and receiver ends

Figure 6: BER versus SNR for 64 QAM constellation with LMS/PTEQ adaptive equalization.

Table 2: BER loss in *dB* for different PTEQ tap lengths L' as compared to the ideal case at SNR = 42 dB, $L = 10$, and $\nu = 8$.

PTEQ taps L'	g_t, ϕ_t	g_r, ϕ_r	$\mathbf{h}_{\text{ti}}$	$\mathbf{h}_{\text{tq}}$	$\mathbf{h}_{\text{ri}}$	$\mathbf{h}_{\text{rq}}$	BER loss in dB
1 (LMS)	0%, 0°	0%, 0°	[1, 0]	[1, 0]	[1, 0]	[1, 0]	2.77
	0%, 0°	5%, 5°	[1, 0]	[1, 0]	[0.9, 0.1]	[0.1, 0.9]	7.64
	5%, 5°	5%, 5°	[0.9, 0.1]	[0.1, 0.9]	[0.9, 0.1]	[0.1, 0.9]	9.26
5	0%, 0°	0%, 0°	[1, 0]	[1, 0]	[1, 0]	[1, 0]	1.96
	0%, 0°	5%, 5°	[1, 0]	[1, 0]	[0.9, 0.1]	[0.1, 0.9]	3.68
	5%, 5°	5%, 5°	[0.9, 0.1]	[0.1, 0.9]	[0.9, 0.1]	[0.1, 0.9]	5.22
10	0%, 0°	0%, 0°	[1, 0]	[1, 0]	[1, 0]	[1, 0]	1.01
	0%, 0°	5%, 5°	[1, 0]	[1, 0]	[0.9, 0.1]	[0.1, 0.9]	1.72
	5%, 5°	5%, 5°	[0.9, 0.1]	[0.1, 0.9]	[0.9, 0.1]	[0.1, 0.9]	2.31
15	0%, 0°	0%, 0°	[1, 0]	[1, 0]	[1, 0]	[1, 0]	0.25
	0%, 0°	5%, 5°	[1, 0]	[1, 0]	[0.9, 0.1]	[0.1, 0.9]	0.83
	5%, 5°	5%, 5°	[0.9, 0.1]	[0.1, 0.9]	[0.9, 0.1]	[0.1, 0.9]	1.09

receiver filter impulse response and also to compensate for the channel and IQ imbalance distortions. The compensation performance depends on how accurately the adaptive equalizer coefficients can converge to the ideal values.

6. CONCLUSION

In this paper, the joint effect of transmitter and receiver frequency-selective IQ imbalance along with channel distortion is studied, and algorithms have been developed to compensate for such distortions. For the case when the cyclic prefix is not sufficiently long to accommodate the channel, transmitter and receiver filter impulse response lengths, a PTEQ-based solution, is proposed. When the cyclic prefix is sufficiently long, the distortions can be compensated by a simple two-tap adaptive equalizer. The algorithms involved correspond to an efficient, post-FFT adaptive equalization which leads to near ideal compensation.

The design of zero-IF receivers typically yields a frequency-independent IQ imbalance on the order of $(g, \phi) = (2-3\%, 2-3^\circ)$ [15]. The performance curves clearly demonstrate that for such IQ imbalance values compensation is absolutely necessary to enable a high data rate communication. It is shown that very large IQ imbalance values can be corrected just as easily. Thus the presented IQ mitigation algorithm allows to greatly relax the zero-IF design specifications.

ACKNOWLEDGMENTS

This research work was carried out at the ESAT laboratory of the Katholieke Universiteit Leuven, in the frame of the Belgian Programme on Inter-university Attraction Poles, initiated by the Belgian Federal Science Policy Office, IUAP P5/11 (mobile multimedia communication systems and networks). The Scientific responsibility is assumed by its authors.

REFERENCES

[1] "IEEE standard 802.11a-1999: wireless LAN medium access control (MAC) & physical layer (PHY) specifications, high-speed physical layer in 5 GHz band," 1999.

[2] I. Koffman and V. Roman, "Broadband wireless access solutions based on OFDM access in IEEE 802.16," *IEEE Communications Magazine*, vol. 40, no. 4, pp. 96–103, 2002.

[3] "ETSI Digital Video Broadcasting; Framing structure, Channel Coding & Modulation for Digital TV," 2004.

[4] A. Baier, "Quadrature mixer imbalances in digital TDMA mobile radio receivers," in *Proceedings of the International Zurich Seminar on Digital Communications. Electronic Circuits and Systems for Communications*, pp. 147–162, Zurich, Switzerland, March 1990.

[5] C.-L. Liu, "Impacts of I/Q imbalance on QPSK-OFDM-QAM detection," *IEEE Transactions on Consumer Electronics*, vol. 44, no. 3, pp. 984–989, 1998.

[6] A. Schuchert, R. Hasholzner, and P. Antoine, "A novel IQ imbalance compensation scheme for the reception of OFDM signals," *IEEE Transactions on Consumer Electronics*, vol. 47, no. 3, pp. 313–318, 2001.

[7] J. Tubbax, B. Côme, L. Van Der Perre, S. Donnay, M. Moonen, and H. De Man, "Compensation of transmitter IQ imbalance for OFDM systems," in *Proceedings of IEEE International Conference on Acoustics, Speech, and Signal Processing (ICASSP '04)*, vol. 2, pp. 325–328, Montreal, Canada, May 2004.

[8] M. Valkama, M. Renfors, and V. Koivunen, "Compensation of frequency-selective I/Q imbalances in wideband receivers: models and algorithms," in *Proceedings of the 3rd IEEE Workshop on Signal Processing Advances in Wireless Communications (SPAWC '01)*, pp. 42–45, Taiwan, China, March 2001.

[9] A. Tarighat, R. Bagheri, and A. H. Sayed, "Compensation schemes and performance analysis of IQ imbalances in OFDM receivers," *IEEE Transactions on Signal Processing*, vol. 53, no. 8, pp. 3257–3268, 2005.

[10] A. Tarighat and A. H. Sayed, "OFDM systems with both transmitter and receiver IQ imbalances," in *Proceedings of the 6th IEEE Workshop on Signal Processing Advances in Wireless Communications (SPAWC '05)*, pp. 735–739, New York, NY, USA, June 2005.

[11] E. Tsui and J. Lin, "Adaptive IQ imbalance correction for OFDM systems with frequency and timing offsets," in *Proceedings of IEEE Global Telecommunications Conference (GLOBECOM '04)*, vol. 6, pp. 4004–4010, Dallas, Tex, USA, November 2004.

[12] K. van Acker, G. Leus, M. Moonen, O. van de Wiel, and T. Pollet, "Per tone equalization for DMT-based systems," *IEEE Transactions on Communications*, vol. 49, no. 1, pp. 109–119, 2001.

[13] D. Tandur and M. Moonen, "Joint compensation of OFDM transmitter and receiver IQ imbalance in the presence of carrier frequency offset," in *Proccedings of European Signal Processing Conference (EUSIPCO '06)*, Florence, Italy, September 2006.

[14] D. Tandur and M. Moonen, "Joint adaptive compensation of transmitter and receiver IQ imbalance under carrier frequency offset in OFDM based systems," to appear in *IEEE Transactions on Signal Processing*, 2007.

[15] B. Côme, D. Hauspie, G. Albasini, et al., "Single-package direct-conversion receiver for 802.1 la wireless LAN enhanced with fast converging digital compensation techniques," in *Proceedings of IEEE MITT-S International Microwave Symposium Digest*, vol. 2, pp. 555–558, Fort Worth, Tex, USA, June 2004.